



Energy Materials Network  
U.S. Department of Energy



**HydroGEN**  
Advanced Water Splitting Materials

# Transformative Materials for High-Efficiency Thermochemical Production of Solar Fuels

**Chris Wolverton**  
**Northwestern University**  
**April 30, 2020**

Project ID P167  
DE-EE0008089

This presentation does not contain any proprietary, confidential, or otherwise restricted information





# Project Overview

## Project Partners

Chris Wolverton, Northwestern University  
Sossina Haile, Northwestern University

## Project Vision

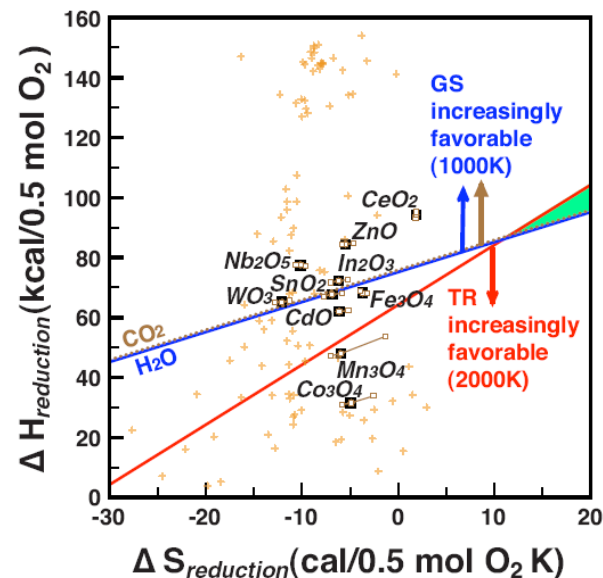
Combine high-throughput computation and experiment to discovery and design novel, improved STCH materials.

## Project Impact

Will explore enormous combinatorial space of materials, to “tune in” desired STCH enthalpy and entropy of reduction. We will design materials with reduced temperatures of reduction but sufficient gas-splitting rates.

|                 |                         |
|-----------------|-------------------------|
| Award #         | EE0008089               |
| Start/End Date  | 10/01/2017 – 03/31/2021 |
| Year 1 Funding* | \$250K                  |
| Year 2 Funding* | \$375K                  |
| Year 3 Funding* | <b>\$ddd</b>            |

*\* this amount does not include cost share or support for HydroGEN resources leveraged by the project (which is provided separately by DOE)*





# Approach- Summary

## Project Motivation

Project builds on background of PIs in STCH materials, attempt to combine high-throughput computational and experimental exploration of oxygen off-stoichiometric oxides and phase change materials for enhancing the efficiency of STC production of solar fuels.

## Barriers

Risk mitigated by exploring large space of novel STCH materials, and the combined use of high-throughput calculations and experimental efforts to explore this space. Focus to date is on perovskite and double-perovskite oxide materials.

## Key Impact

Identify compounds which show: a) synthesizability, b) thermodynamics favorable for  $<1400^{\circ}\text{C}$  reduction and c) thermodynamics favorable for facile water splitting. State-of-the-art currently  $\text{CeO}_2$  and SLMA perovskite.

## Partnerships

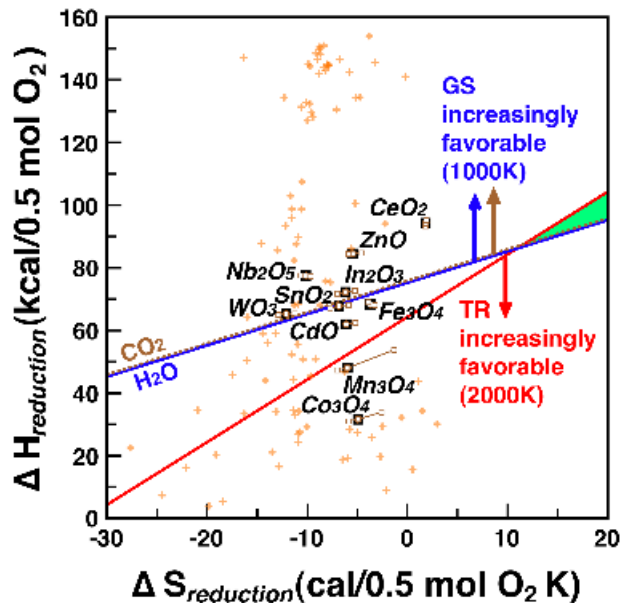
Productive collaborations with HydroGEN nodes and other seedling projects: Ginley (NREL) – in situ XRD and synthesis; Zakutayev (NREL) – thin film composition gradient synthesis; McDaniel/Coker (SNL) high-T XRD; O'Hayre (CSM) –  $(\text{Sr,Ce})_2\text{MnO}_4$  layered perovskite



# Approach- Innovation

## A Design Map for Materials:

Thermodynamics very challenging for stoichiometric reactions (at moderate pressure)



need moderate enthalpy and high entropy

B. Meredig and C. Wolverton, *Phys. Rev. B.* 80, 245119 (2009) (Data from SSUB database)

## Perovskites ( $ABO_3$ or $AA'BB'O_6$ )

- ✓ Until recently : ceria ( $CeO_2$ ) [1]
- ✓ More recently: perovskites [2]
- ✓ Perovskites have several good qualities for TWS
  - Tolerate large oxygen off-stoichiometry
  - High Stability
  - Studied for other applications (e.g. SOFC)



- ✓ Enormous compositional space
- ✓ **High-Throughput Density Functional Theory,** The Open Quantum Materials Database (OQMD)
- ✓ High-Throughput screening of ~11,000  $ABO_3$  perovskites based on **stability and reduction enthalpy**

[1] W.C. Chueh, et. al, *Science* 330 (2010)

[2] A.H. McDaniel, et.al, *Energy & Environmental Science* 6, 2424 (2013)

[3] S. Kirklin, et. al, *npj Computational Materials* 1, 15010 (2015)



## Summary of Year-2 Scope of Work

- (a) Evaluate thermodynamics of site-substituted perovskites with electrochemical impedance measurement using thin film
- (b) Experimentally measure thermodynamics of reduction of seven predicted double-perovskite oxides and their applicability for STCH
- (c) Expand computational double perovskite survey to 10,000's of compounds
- (d) Validation of computational entropies for materials screening

The thermodynamics acquired from electrochemical impedance measurement on thin film will be discussed, the synthesis, thermodynamics of reduction and hydrogen production measurement on predicted double perovskites will be presented. The expanded computational searching for double perovskite and the validated entropy computation models will be useful for identifying more promising materials for STCH.



# Relevance & Impact

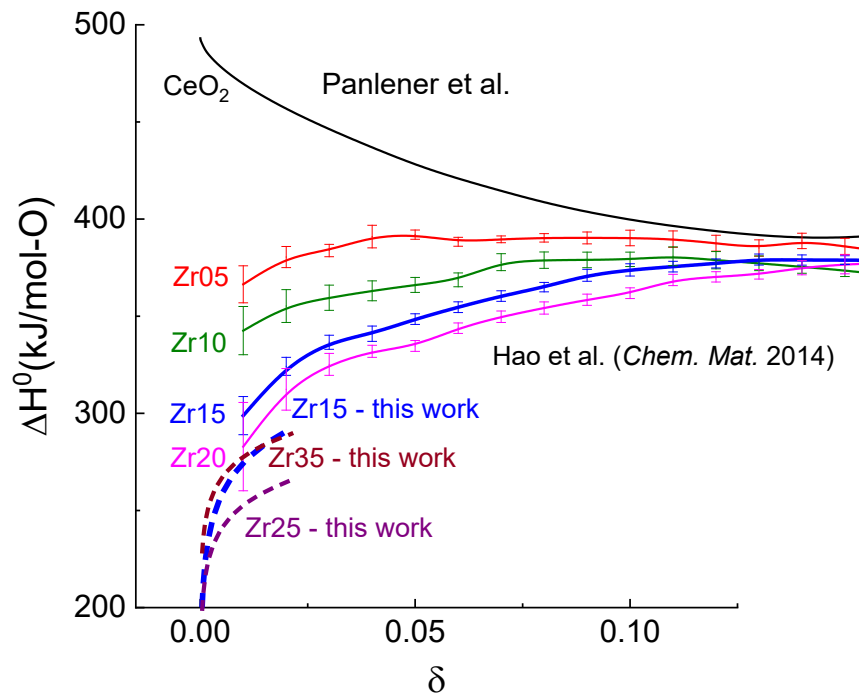
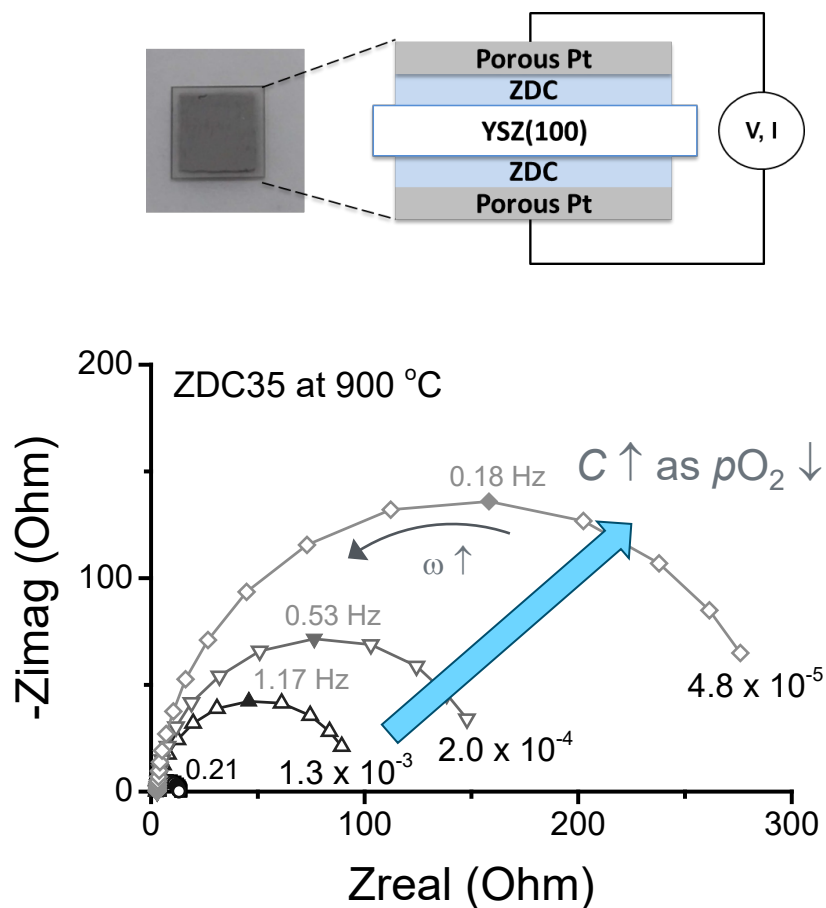
- This project aims to identify promising compounds which show:
  - a) ground state stability/synthesizeability of compound,
  - b) thermodynamics favorable for <1400C reduction and
  - c) thermodynamics favorable for facile water splitting.

State-of-the-art currently  $\text{CeO}_2$  and SLMA perovskite.

- Discovery of new, higher-efficiency materials is critical towards the practical use of STCH for  $\text{H}_2$  production (and solar fuels, more generally). ***Our combined high-throughput computation and experimental approach is greatly accelerating this materials discovery effort.***
- ***Collaborations with HydroGEN nodes (NREL, SNL) and other Seedling projects (CSM) will greatly facilitate research progress***



# Accomplishments – Oxide Thermochemistry by Thin Film Electrochemical Impedance in Year 1



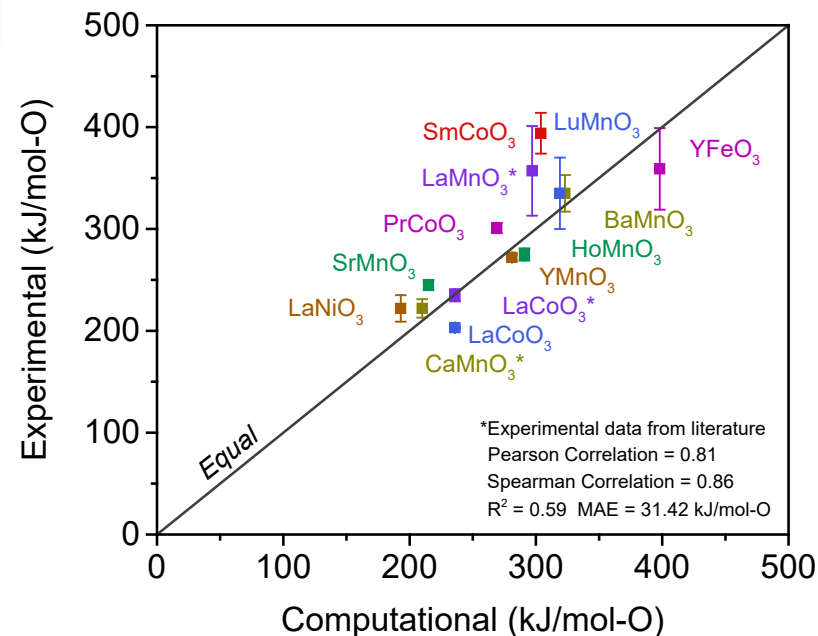
- Exquisite access to low  $\delta$  region
- Not possible to measure by TGA
- Important for assessing entropy

Method demonstrated using zirconia-ceria films, lessons learned for improvement



# Accomplishments – Reduction of Oxide Materials in Year-1

| Material           | Structure Type        | Crystal System | Space Group          |
|--------------------|-----------------------|----------------|----------------------|
| LuFeO <sub>3</sub> | Perovskite            | Orthorhombic   | Pbnm                 |
| HoFeO <sub>3</sub> | Perovskite            | Orthorhombic   | Pbnm                 |
| YFeO <sub>3</sub>  | Perovskite            | Orthorhombic   | Pnma                 |
| LuCrO <sub>3</sub> | Perovskite            | Orthorhombic   | Pbnm                 |
| ErCrO <sub>3</sub> | Perovskite            | Orthorhombic   | Pbnm                 |
| HoCrO <sub>3</sub> | Perovskite            | Orthorhombic   | Pbnm                 |
| PrCoO <sub>3</sub> | Perovskite            | Orthorhombic   | Pbnm                 |
| SmCoO <sub>3</sub> | Perovskite            | Orthorhombic   | Pbnm                 |
| LaCoO <sub>3</sub> | Perovskite            | Rhombohedral   | R-3c                 |
| LaNiO <sub>3</sub> | Perovskite            | Rhombohedral   | R-3c                 |
| YMnO <sub>3</sub>  | “LuMnO <sub>3</sub> ” | Hexagonal      | P6 <sub>3</sub> mc   |
| LuMnO <sub>3</sub> | “LuMnO <sub>3</sub> ” | Hexagonal      | P6 <sub>3</sub> mc   |
| HoMnO <sub>3</sub> | “LuMnO <sub>3</sub> ” | Hexagonal      | P6 <sub>3</sub> mc   |
| SrMnO <sub>3</sub> | “BaMnO <sub>3</sub> ” | Hexagonal      | P6 <sub>3</sub> /mmc |
| BaMnO <sub>3</sub> | ”BaNiO <sub>3</sub> ” | Hexagonal      | P6 <sub>3</sub> /mmc |
| CaMnO <sub>3</sub> | Perovskite            | Ortho          | Pnma                 |
| LaMnO <sub>3</sub> | Perovskite            | Orthorhombic   | Pnma                 |



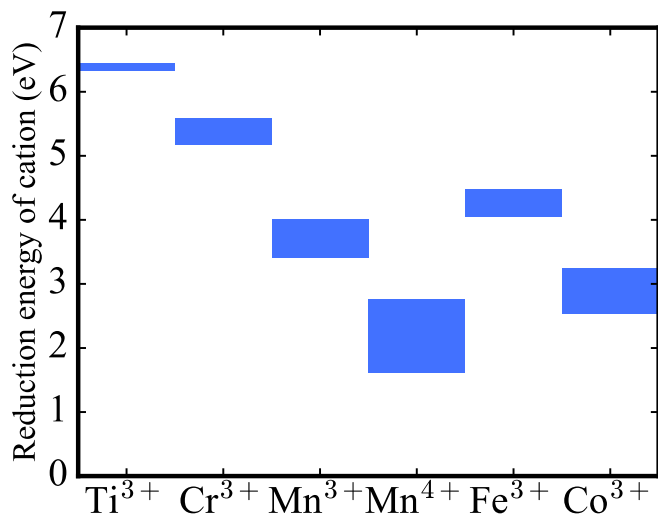
Experimental measurements of redox thermodynamics of computationally predicted perovskites by TGA

- (i) Validate the enthalpy calculation
- (ii) Obtain high-quality entropy data to guide entropy calculation



# Accomplishments – Synthesis and Reduction of Oxide Materials in Year-2

## Mn-Containing $A_2BB'O_6$



| Compounds     | Structure | $E_V^0$ (eV/vacancy) |
|---------------|-----------|----------------------|
| $Sr_2TiMnO_6$ | P21/c     | 2.190                |
| $La_2CuMnO_6$ | P21/c     | 2.892                |
| $La_2ZnMnO_6$ | P21/c     | 3.031                |
| $Sr_2CuWO_6$  | Fm-3m     | 3.071                |
| $Sr_2CuWO_6$  | I4/m      | 3.111                |
| $Sr_2ZrMnO_6$ | Fm-3m     | 3.270                |
| $La_2NiMnO_6$ | P21/c     | 3.438                |

## Objective

### (1) Experimental:

- Target enthalpy in the range 150 – 300 kJ/mol-O
- intermediate composition perovskites w/tunable capacity, releasing 5 mL  $O_2$  g<sup>-1</sup>(oxide)

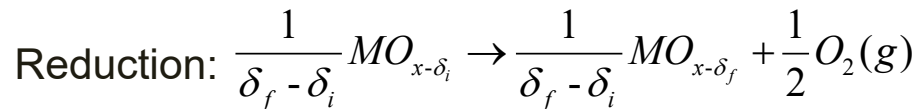
### (2) Computational:

- a database of >  $10^4$  site-substituted  $AA'BB'O_6$  perovskites and double perovskites
- entropy calculation within 20% of experimental



# Accomplishments – Thermodynamic Measurements

- 7 predicted  $A_2BB'O_6$  compounds were synthesized and temperature stability range of each material was evaluated
- Thermogravimetry (TG) was employed to measure oxygen non-stoichiometry at different oxygen partial pressures and temperatures, and the reduction enthalpy and entropy were extracted



When at Equilibrium:  $\Delta G = \Delta G^0 + RT \ln(K^{eq}) = 0$

$$K^{eq} = pO_2^{1/2} = \exp\left(-\frac{\Delta G^0}{RT}\right) = \exp\left(-\frac{\Delta H^0 - T\Delta S^0}{RT}\right)$$

$$\frac{R}{2} \ln(pO_2) = -\frac{\Delta H^0}{T} + \Delta S^0$$

For a given  $\delta$ , linear relation of  $\frac{R}{2} \ln(pO_2)$  vs.  $\frac{1}{T}$  gives slope =  $-\Delta H^0$ , intercept =  $\Delta S^0$

**$\Delta H$  and  $\Delta S$  control T, P for water splitting**

**Also, provides key data for prediction of hydrogen evolution**

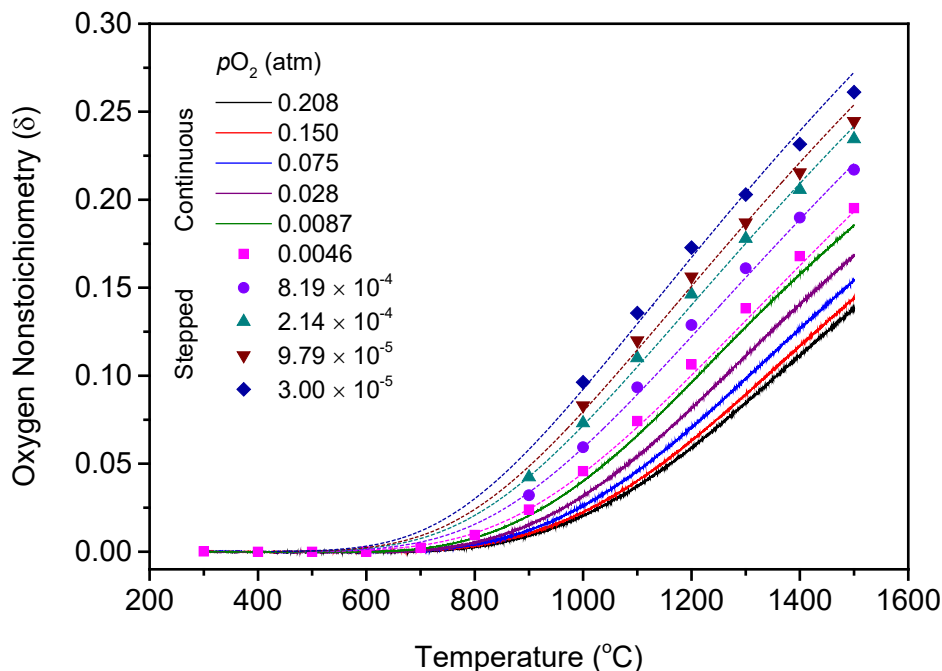


# Accomplishments – Oxygen Non-stoichiometry

## Overall $\delta(T)$ of Representative Materials

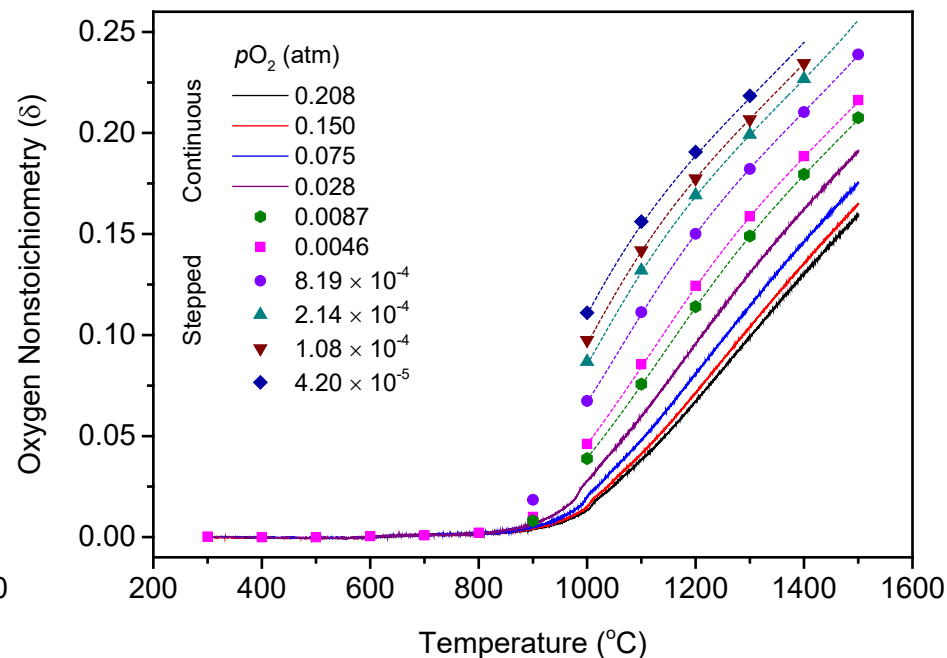
Oxygen non-stoichiometry profiles from continuous and stepped TGA analysis

### Material A



Analyze within  $0.004 < \delta < 0.245$

### Material B



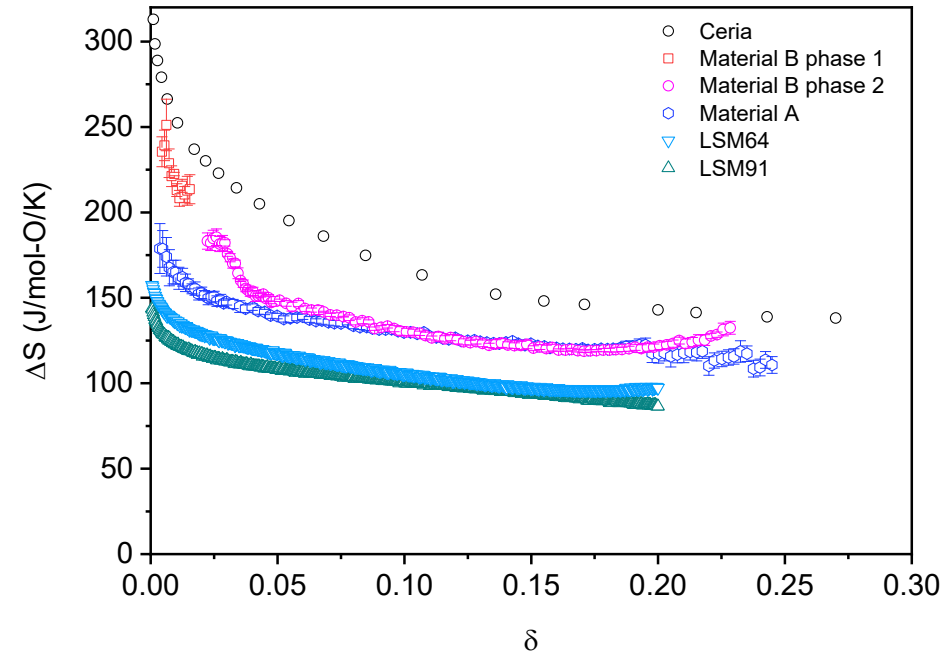
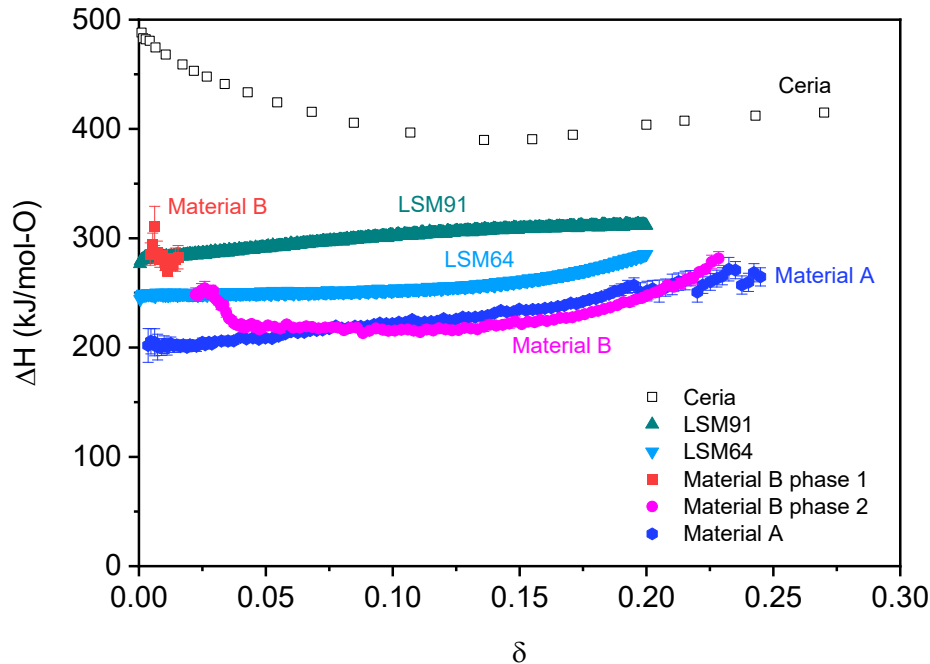
Analyze within  $0.004 < \delta < 0.228$



# Accomplishments – $\Delta H$ and $\Delta S$ of Reduction

## Thermodynamics of Reduction

The enthalpy and entropy are extracted using van't Hoff method<sup>[1,2]</sup> and compared with other STCH materials



- Enthalpy of Materials A and B (two phases) all fall in the range of 150 – 300 kJ/mol-O
- Lower enthalpy and higher entropy compared to typical perovskite  $\text{La}_{1-x}\text{Sr}_x\text{MnO}_3$ , thermodynamically more favorable for water splitting

[1] Panlener, R. J., et al., Journal of Physics and Chemistry of Solids, 1975.

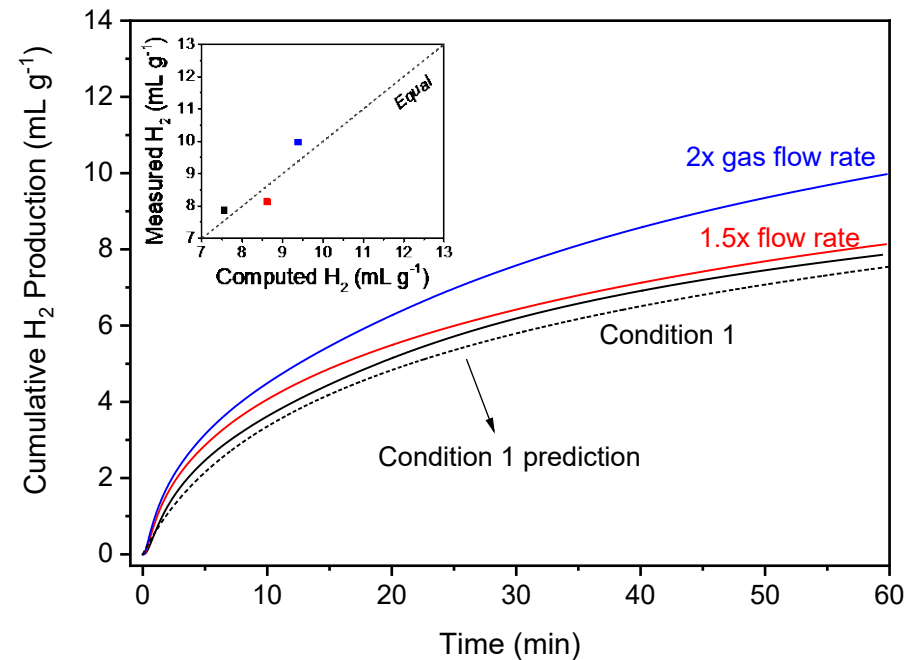
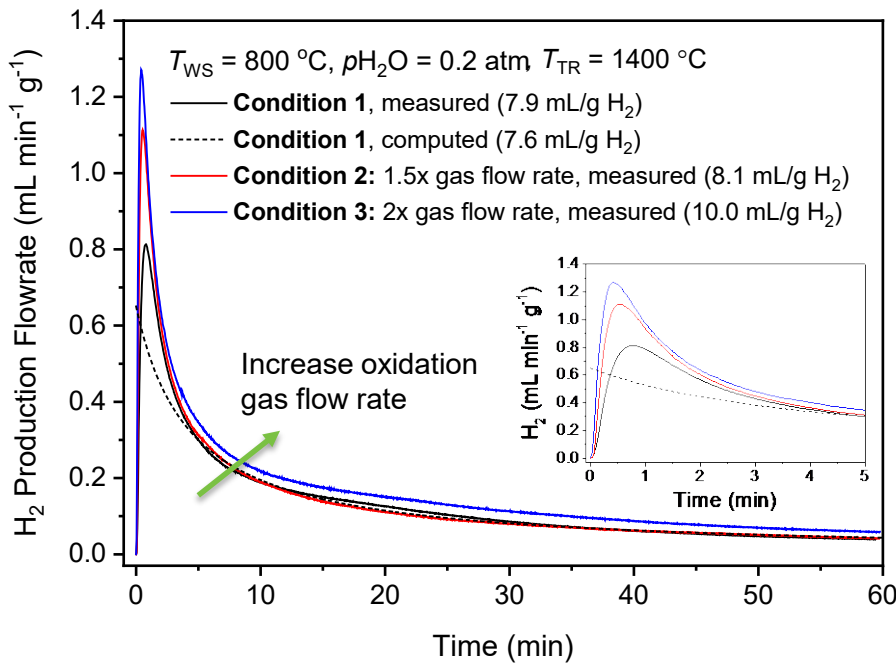
[2] Hao, Y., et al., Chemistry of Materials, 2014.



# Accomplishments – Examples of Predictable Hydrogen Production using Thermodynamics Data

## Predictable Hydrogen Productions

Compare measured hydrogen production profiles to profiles predicted for a gas flow or thermodynamically limited process <sup>[1,2]</sup> (solid remains in quasi-equilibrium with gas phase)



Profiles are very sensitive to gas flow rate, as predicted for quasi-equilibrium H<sub>2</sub> production can be reasonably well predicted using thermodynamic data  
Macroscopic rate is limited by thermodynamics, minor role of material kinetics

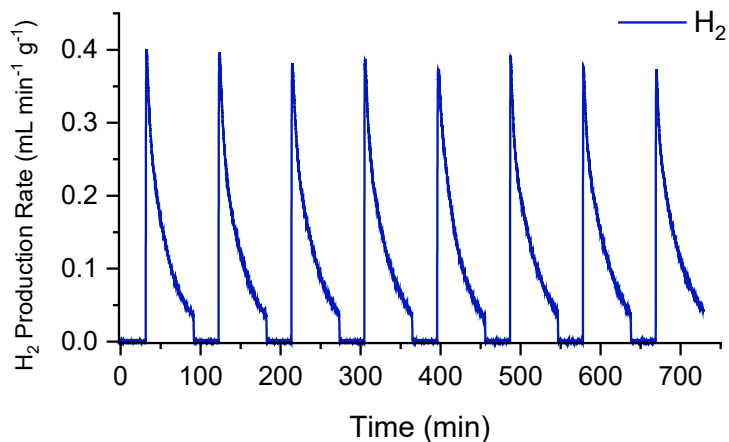
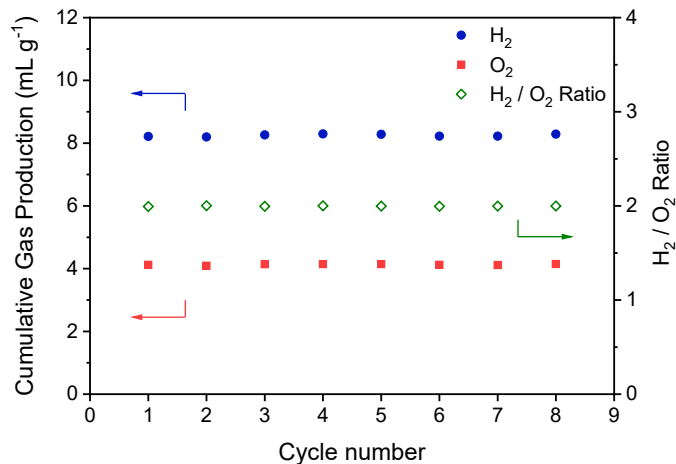
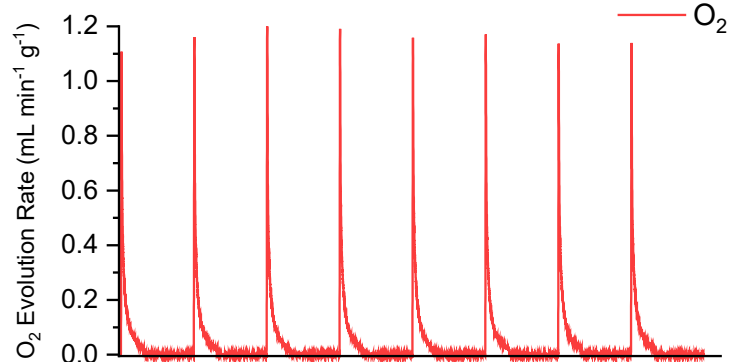
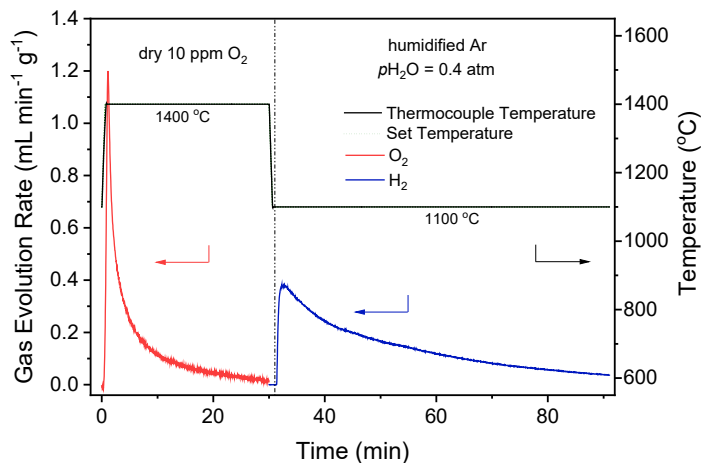


# Accomplishments – Cyclic Hydrogen Production

## H<sub>2</sub> Production using Material A

1400 °C – 1100 °C,  $p_{H_2O} = 0.4 \text{ atm}$

**Average H<sub>2</sub>: 8.25 mL/g-oxide**



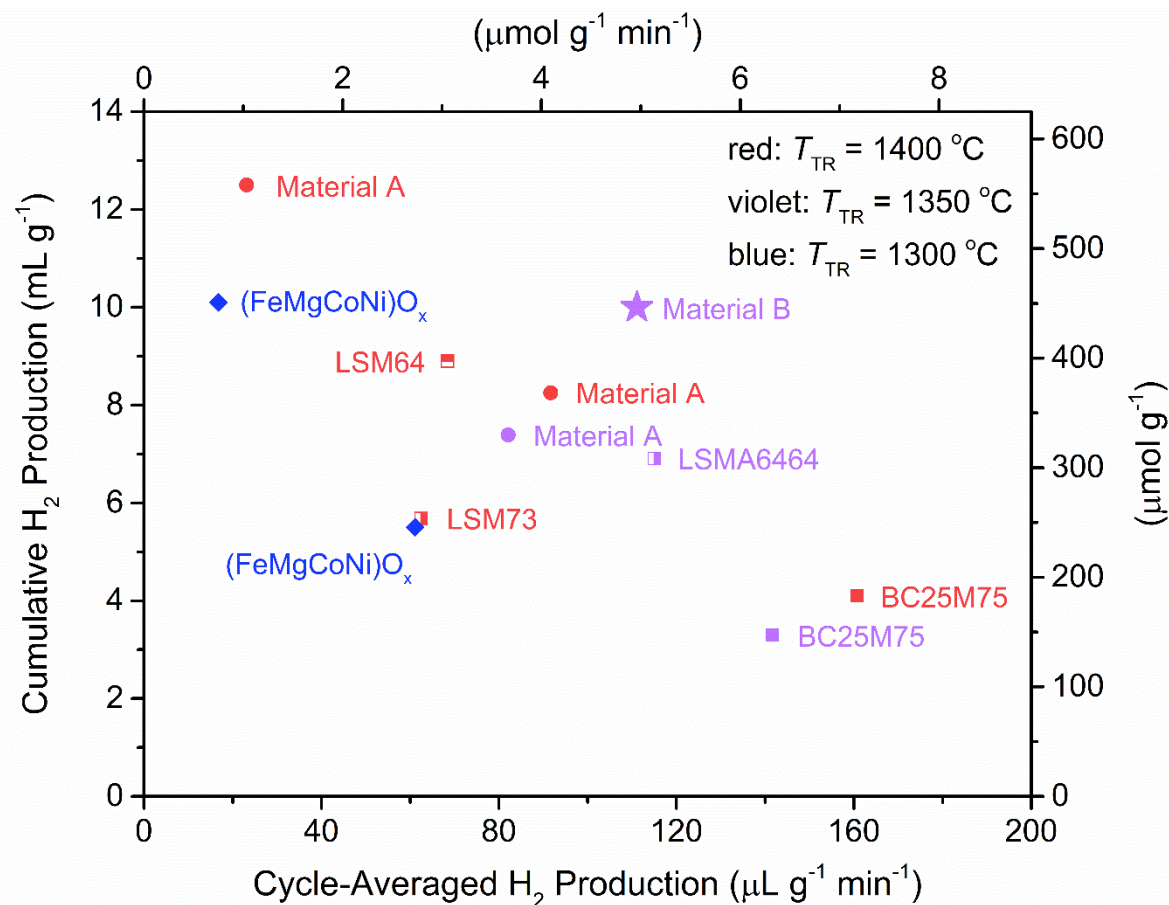
Free of (short term) degradation; ideal ratio of 2:1 in H<sub>2</sub>:O<sub>2</sub> observed



# Accomplishments – Hydrogen Productivity Comparison with Literature Results

## H<sub>2</sub> Productivity Comparison

Compared with reported promising materials on the basis of cumulative hydrogen productivity versus cycle-time-averaged productivity



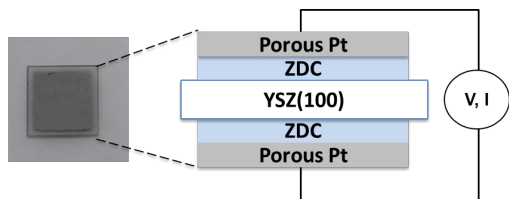
Our materials A and B offer excellent combinations of cumulative and cycle-average hydrogen productivity

A and B are competitive candidates for high-capacity thermochemical hydrogen production

(FeMgCoNi)O<sub>x</sub>, Zhai (*E&ES*, 2018)  
SM64 (= La<sub>0.6</sub>Sr<sub>0.4</sub>MnO<sub>3</sub>) Yang (*J. Mat. Chem. A*, 2014).  
SM74 (= La<sub>0.7</sub>Sr<sub>0.3</sub>MnO<sub>3</sub>) ibid  
SMA6464 (= La<sub>0.6</sub>Sr<sub>0.4</sub>Mn<sub>0.6</sub>Al<sub>0.4</sub>O<sub>3</sub>), McDaniel (*E&ES*, 2013)  
BC25Mn75 (BaCe<sub>0.25</sub>Mn<sub>0.75</sub>O<sub>3</sub>), Barcellos (*E&ES*, 2018)



# Accomplishments – Thin Film Characterization



$$C_{total}^{film} = C_{chem} + C_{int} = 2C_{meas}^{synn}$$

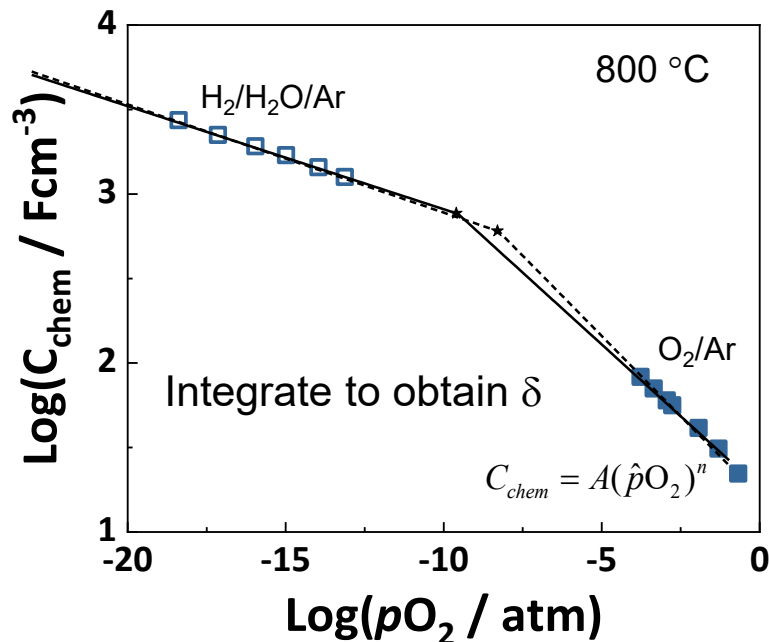
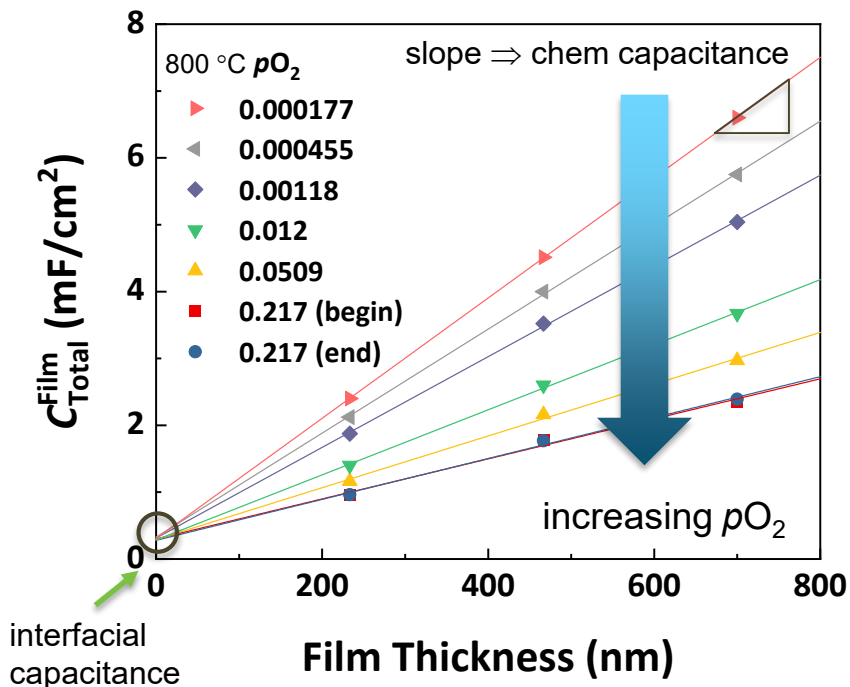
$\propto L$                        $\neq f(L)$

$$C_{chem} = -\frac{8F^2 V \delta}{RTV_m} \left( \frac{d \ln \delta}{d \ln(\hat{p}O_2)} \right)$$

volume

Vary thickness to distinguish contributions

Example:  $Ce_{0.8}Zr_{0.2}O_{2-\delta}$

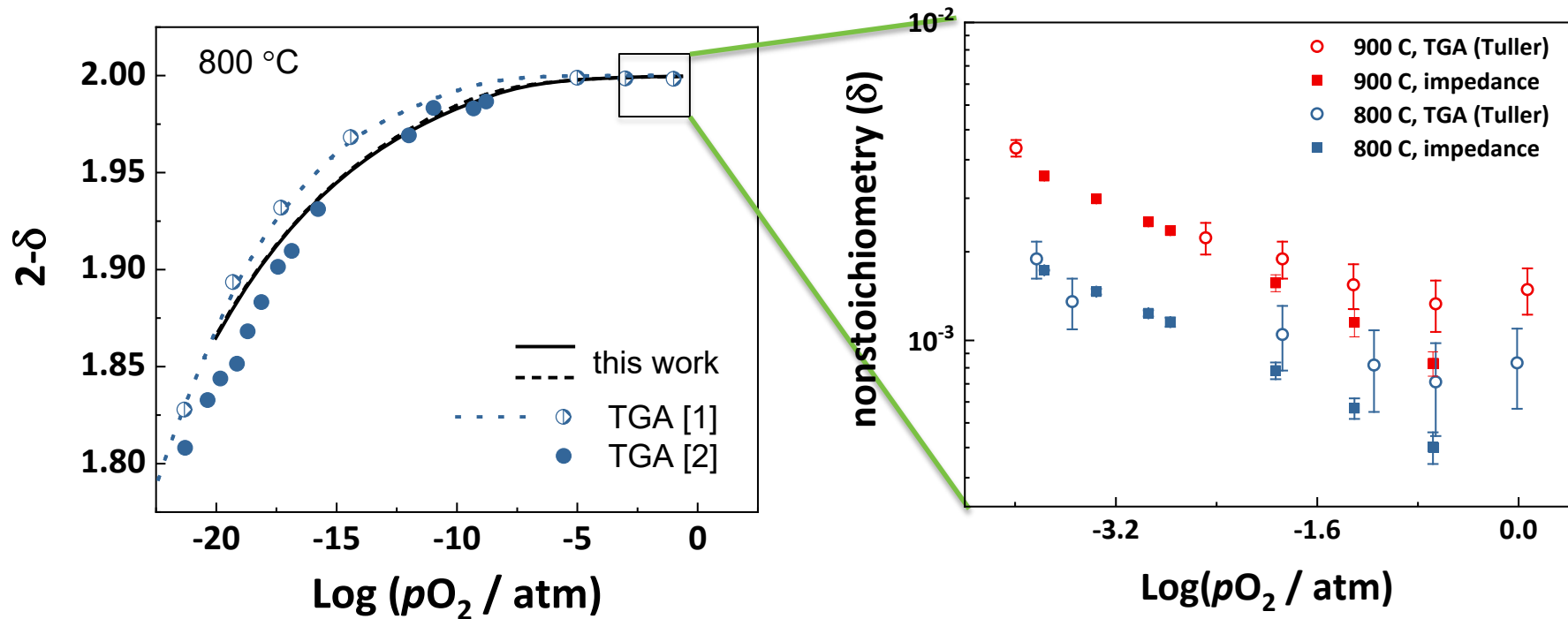




# Accomplishments – Thin Film Characterization

$$d\delta = -\frac{RTV_m}{8F^2V} \frac{C_{chem}}{\hat{p}O_2} d(\hat{p}O_2)$$

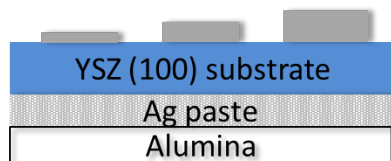
integrate to obtain  $\delta$



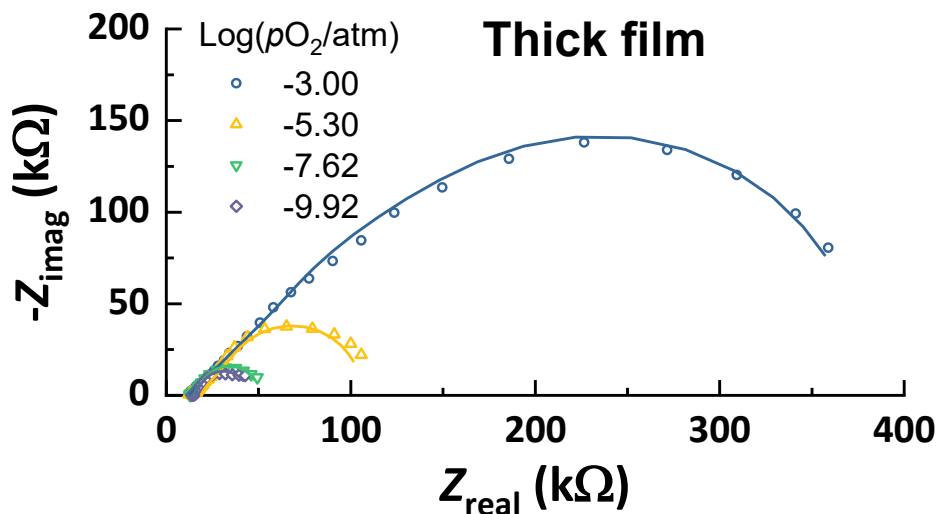


# Accomplishments – Thin Film Characterization

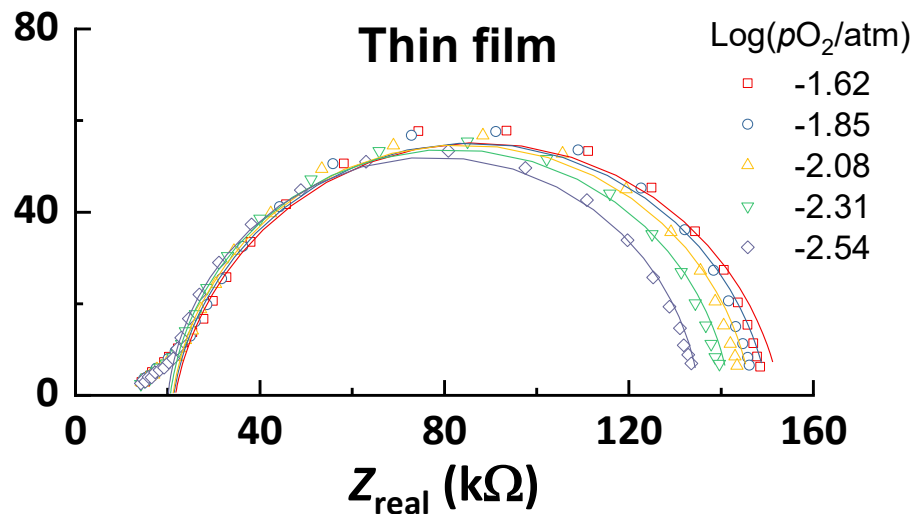
## Material A



Apply bias in microdot geometry to achieve arbitrary effective  $pO_2$   
No longer limited to gas mixtures



$t \sim 500$  nm,  $T = 600$  °C

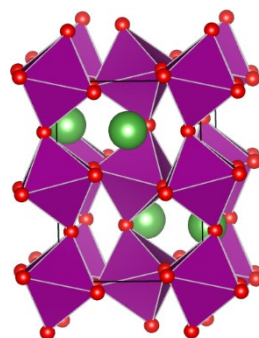
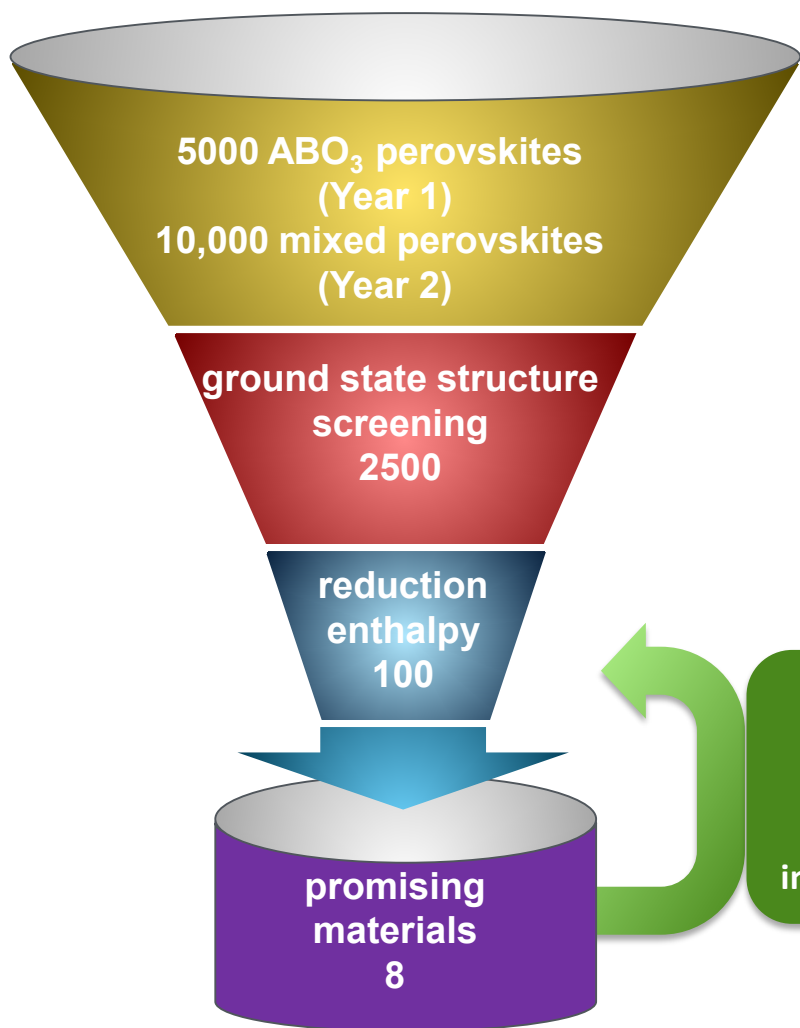


$t \sim 40$  nm,  $T = 580$  °C

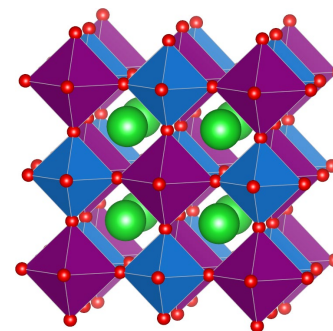
Difference in spectra features  $\Rightarrow$  bulk transport properties also accessible



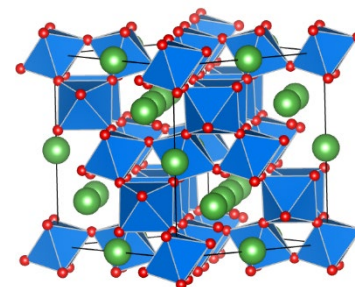
# Accomplishments: High throughput DFT screening



perovskite



mixed perovskite



pyrochlore

Use experimental  
information to refine  
computational predictive  
accuracy (structural  
information, value of U, etc.)



# Accomplishments: HT DFT screening mixed perovskite

**Expand computational mixed-/double-perovskite survey to 10,000's of compounds**

We performed HT DFT screening on stabilities of

- 1)  $A_2BB'O_6$  ( $A=Ca, Sr, Ba, La, Zn, Cd, Hg,$  and  $Pb$ ;  $B/B'=50$  elements) mixed  $B$ -site perovskites. There are 1250 possible combinations for each  $A$ -site cation. *Ten* prototype structures for compounds with  $A=Ca, Sr, Ba,$  and  $La$  to determine the ground state structure. *One* prototype structures for compounds with  $A=Zn, Cd, Hg,$  and  $Pb$
- 2)  $RAB_2O_6$  ( $R=Y$  + rare earth,  $A=$ alkaline earth metal, transition metal) mixed  $A$ -site perovskites

**Two** prototype structures for 1750 compositions  
27 of them are stable and 135 are metastable

| A     |    | B/B' |    | X   |    | B    |    | O   |    |    |    |    |    |    |    |    |
|-------|----|------|----|-----|----|------|----|-----|----|----|----|----|----|----|----|----|
| Green |    | Blue |    | Red |    | Blue |    | Red |    |    |    |    |    |    |    |    |
| Li    | Be |      |    |     |    |      | B  |     | O  |    |    |    |    |    |    |    |
| Na    | Mg |      |    |     |    | Al   | Si |     |    |    |    |    |    |    |    |    |
| K     | Ca | Sc   | Ti | V   | Cr | Mn   | Fe | Co  | Ni | Cu | Zn | Ga | Ge | As | Se | Br |
| Rb    | Sr | Y    | Zr | Nb  | Mo | Tc   | Ru | Rh  | Pd | Ag | Cd | In | Sn | Sb | Te | I  |
| Cs    | Ba | La   | Hf | Ta  | W  | Re   | Os | Ir  | Pt | Au | Hg | Tl | Pb | Bi |    |    |

**Total number of structures calculated: 38673**

**Total number of compositions screened: 11750**



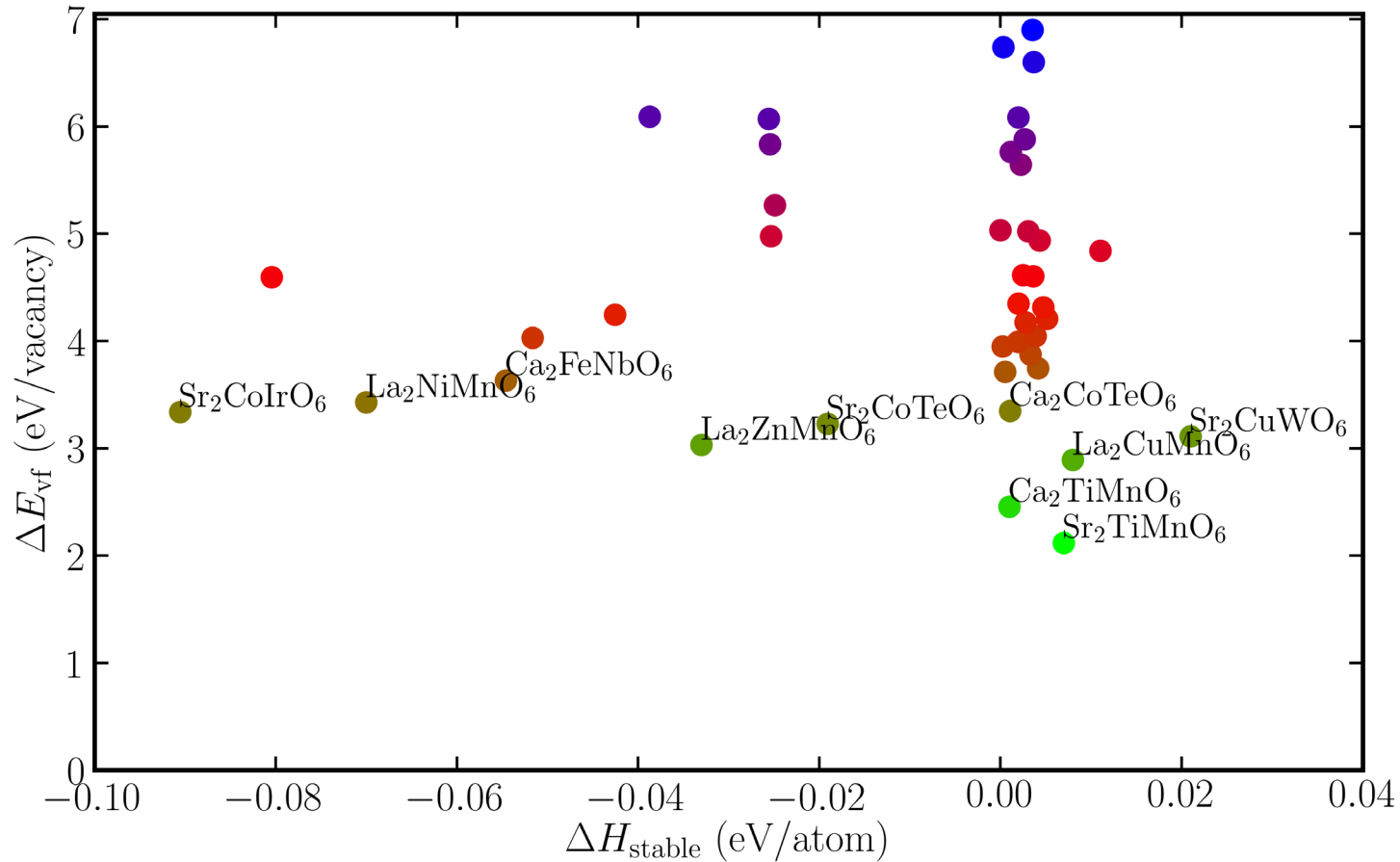
# Accomplishments: HT DFT screening mixed perovskite

| A-site | Stable | Metastable | Experimentally known    |                         |
|--------|--------|------------|-------------------------|-------------------------|
|        |        |            | not in OQMD             | in OQMD                 |
|        |        |            | total/stable/metastable | total/stable/metastable |
| Ba     | 216    | 199        | 75/46/21                | 47/40/7                 |
| Sr     | 187    | 212        | 77/44/26                | 52/46/6                 |
| Ca     | 109    | 250        | 67/35/29                | 21/17/2                 |
| La     | 63     | 181        | 56/15/31                | 32/18/13                |
| Zn     | 0      | 16         | 0                       | 0                       |
| Cd     | 5      | 52         | 6/1/2                   | 1/1/0                   |
| Hg     | 1      | 11         | 0                       | 1/1/0                   |
| Pb     | 18     | 118        | 67/2/39                 | 7/2/5                   |

- Most experimentally known mixed/double perovskites determined to be stable or metastable: Validation of our screening strategy
- ***Significant number of previously-unknown mixed perovskites predicted***



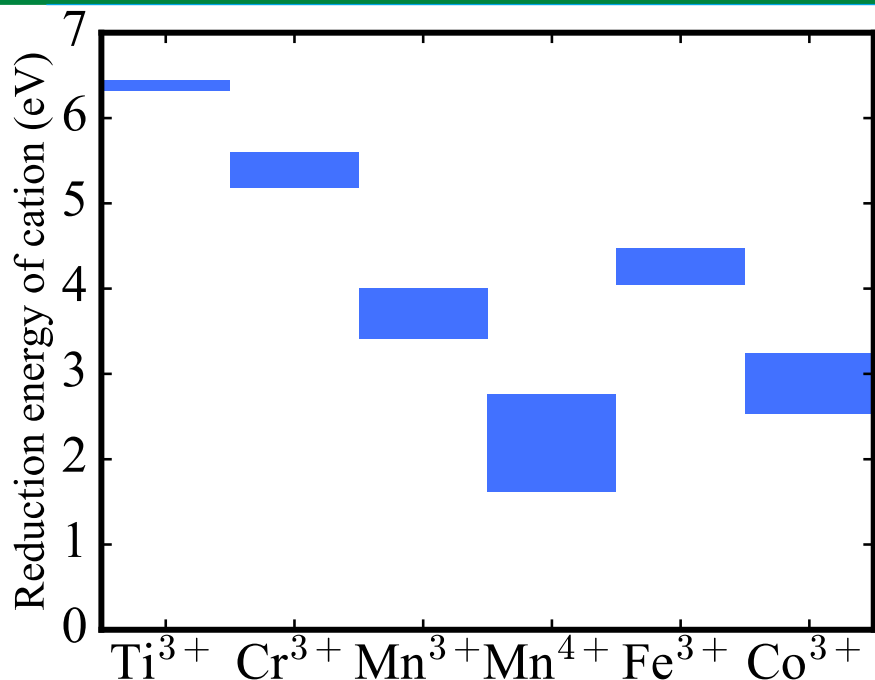
# Accomplishments: HT DFT screening mixed perovskite



- Oxygen vacancy formation energy of the double perovskites that have been synthesized experimentally
- Some calculations of newly discovered compounds still ongoing



# Accomplishments: HT DFT screening mixed perovskite

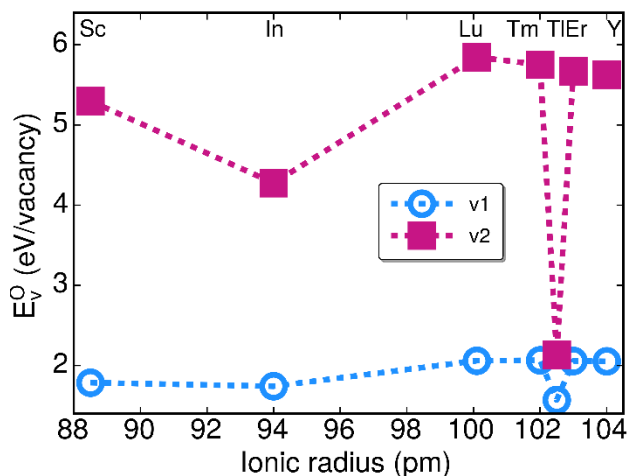


| Compounds                          | Structure               | $E_V^0$ (eV/vac.) |
|------------------------------------|-------------------------|-------------------|
| Sr <sub>2</sub> TiMnO <sub>6</sub> | <i>P2<sub>1</sub>/c</i> | 2.117             |
| Ca <sub>2</sub> TiMnO <sub>6</sub> | <i>P2<sub>1</sub>/c</i> | 2.455             |
| La <sub>2</sub> CuMnO <sub>6</sub> | <i>P2<sub>1</sub>/c</i> | 2.892             |
| Sr <sub>2</sub> HfMnO <sub>6</sub> | <i>P2<sub>1</sub>/c</i> | 2.910             |
| Ca <sub>2</sub> ZrMnO <sub>6</sub> | <i>P2<sub>1</sub>/c</i> | 2.930             |
| La <sub>2</sub> ZnMnO <sub>6</sub> | <i>P2<sub>1</sub>/c</i> | 3.031             |
| Ca <sub>2</sub> HfMnO <sub>6</sub> | <i>P2<sub>1</sub>/c</i> | 3.090             |
| Sr <sub>2</sub> CuWO <sub>6</sub>  | <i>Fm-3m</i>            | 3.071             |
| Sr <sub>2</sub> CuWO <sub>6</sub>  | <i>I4/m</i>             | 3.111             |
| Sr <sub>2</sub> ZrMnO <sub>6</sub> | <i>Fm-3m</i>            | 3.270             |
| La <sub>2</sub> NiMnO <sub>6</sub> | <i>P2<sub>1</sub>/c</i> | 3.438             |
| Sr <sub>2</sub> ZrMnO <sub>6</sub> | <i>P2<sub>1</sub>/c</i> | 4.348             |

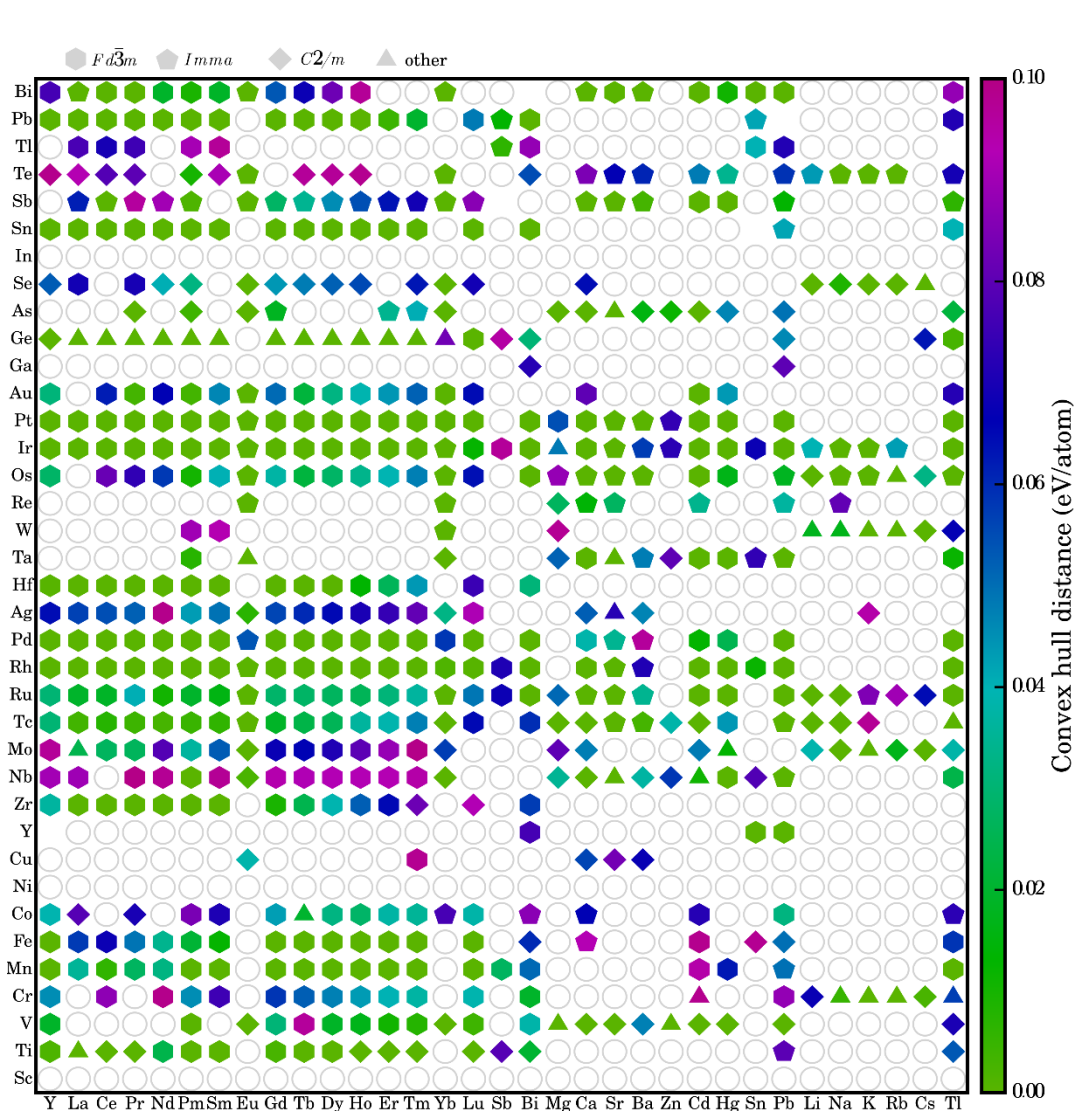
- Among the transition metal of *B*-sit cation coordinated in oxygen octahedral, we found Mn<sup>4+</sup> is much easier to reduce than other cations. The spread of the value is mainly from the effects of octahedral distortion.
- Therefore, we performed DFT calculations on known and predicted stable Mn<sup>4+</sup> containing double perovskites, and found the oxygen vacancy formation energy varies from 2.2 to 3.4 eV/vacancy, depending on another *B*-site cation and octahedral rotation



# Accomplishments: HT DFT screening pyrochlore



Our calculations show that one oxygen site of  $R_2Mn_2O_7$  pyrochlore compounds have relatively low oxygen vacancy formation energy. Pyrochlore also has high oxygen diffusivity. Therefore, we performed HT DFT screening on thermodynamic stability of pyrochlore





# Compute Entropies of Reduction

- Compute entropies of reduction of experimentally measured perovskites and double-perovskites
- *Question: Which entropy contributions are most significant? Specifically, does vibrational entropy make a significant contribution?*

Formation free-energy ( $\Delta G$ ) of oxygen vacancy:

$$\Delta G(T) = \Delta E + \Delta H^{\text{vib}}(T) - T[\Delta S^{\text{vib}}(T) + \Delta S^{\text{conf}}(T) + \Delta S^{\text{electron}}(T)] + 0.5 * TS(\text{O}_2)$$

$\Delta E$  - vacancy formation enthalpy

$\Delta H^{\text{vib}}$  - vibrational energy

$\Delta S^{\text{vib}}$  - vibrational entropy

$\Delta S^{\text{conf}}$  - configurational entropy

$\Delta S^{\text{electron}}$  - electronic entropy

$S(\text{O}_2)$  - entropy of  $\text{O}_2$  gas (JANAF)

We calculated configurational and vibrational entropies difference of bulk and its defective counterpart. The vibrational entropy calculation requires phonon calculations, which is very expensive. We spent several million CPU hours on vibrational entropy calculations.



# Compute Entropies of Reduction: Issues

1. Phonon calculation is very expensive, especially for the supercell with vacancy. For example, one phonon calculation within the harmonic approximation for the vacancy takes ~500,000 CPU hours
2. For compounds with a low-temperature distorted structure (which commonly happens in perovskite), the room-temperature phase usually has imaginary frequencies, which prevents vibrational entropy calculations. For example, DFT calculations of the 4-H structure of  $\text{SrMnO}_3$  synthesized experimentally, has many imaginary frequencies, since there is a phase transition to  $C222_1$  phase at low temperature.
3. The simplest method that can include the temperature effect on phonon calculations is the self-consistent phonon, which is 10 ~ 50 times more expensive than harmonic phonon calculations.

Therefore, we only calculated the vibrational entropies of the compounds without imaginary frequencies.

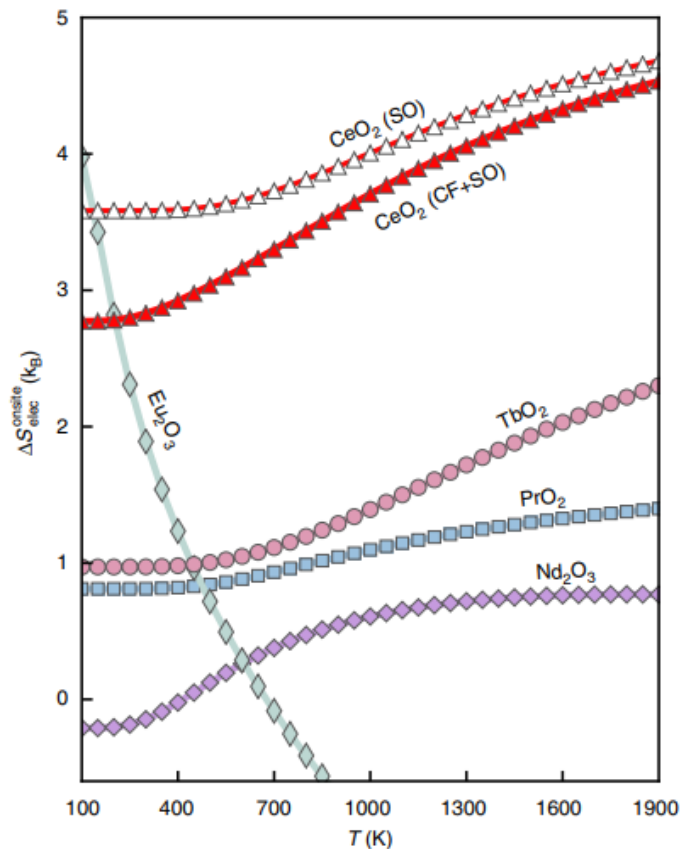


# Experimental vs. Computational Entropy of Reduction (T= 1000 K)

| ABO <sub>3</sub>   | $\frac{1}{2} S(O_2)$<br>[J/mol/K] | $\Delta S_{conf}$<br>[J/mol/K] | $\Delta S_{vib}$ (V)<br>[J/mol/K] | $\Delta S_{calc}$<br>[J/mol/K] | $\Delta S_{exp}$<br>[J/mol/K] | Comments            |
|--------------------|-----------------------------------|--------------------------------|-----------------------------------|--------------------------------|-------------------------------|---------------------|
| LaCoO <sub>3</sub> | 122                               | 32                             |                                   |                                | 167 ± 2                       | Magmom issues       |
| PrCoO <sub>3</sub> | 122                               | 31                             |                                   |                                | 218 ± 4                       | Magmom issues       |
| SmCoO <sub>3</sub> | 122                               | 32                             |                                   |                                | 288 ± 7                       | Magmom issues       |
| YFeO <sub>3</sub>  | 122                               | 27                             | -1                                | 148                            | 163 ± 20                      | <b>Within 20% ✓</b> |
| BaMnO <sub>3</sub> | 122                               | 32                             |                                   |                                | 220 ± 14                      | Imaginary phonons   |
| CaMnO <sub>3</sub> | 122                               | 31                             | 18                                | 171                            | 188 ± 9                       | <b>Within 20% ✓</b> |
| HoMnO <sub>3</sub> | 122                               | 33                             | 12                                | 167                            | 166 ± 9                       | <b>Within 20% ✓</b> |
| LaMnO <sub>3</sub> | 122                               | 29                             |                                   |                                | 155 ± 42                      | Complex structure   |
| LuMnO <sub>3</sub> | 122                               | 33                             |                                   |                                | 197 ± 22                      | In progress         |
| SrMnO <sub>3</sub> | 122                               | 32                             |                                   |                                | 166 ± 3                       | Imaginary phonons   |
| YMnO <sub>3</sub>  | 122                               | 33                             | 11                                | 166                            | 161 ± 4                       | <b>Within 20% ✓</b> |
| LaNiO <sub>3</sub> | 122                               | 32                             |                                   |                                | 186 ± 14                      | In progress         |



# Search for $\text{Ce}^{4+}$ oxides for STCH application



The giant onsite electronic entropy of  $\text{Ce}^{4+} \rightarrow \text{Ce}^{3+}$  motivates us to search for other  $\text{Ce}^{4+}$  oxides with smaller reduction enthalpy

| Comp.  | source      | Space group        | $E_v^0$ (eV/vacancy)    |
|--|-------------|--------------------|-------------------------|
| $\text{CeO}_2$                               | ICSD        | <i>Fm-3m</i>       | 3.05                    |
| <b><math>\text{CeTi}_2\text{O}_6</math></b>  | <b>ICSD</b> | <b><i>C2/m</i></b> | <b>2.59, 2.43, 2.52</b> |
| $\text{Sr}_2\text{CeO}_4$                    | ICSD        | <i>Pbam</i>        | 5.01, 4.95              |
| $\text{SrCeO}_3$                             | ICSD        | <i>Pnma</i>        | 4.34, 4.39              |
| $\text{BaCeO}_3$                             | ICSD        | <i>Pnma</i>        | 4.67, 4.68              |
| $\text{CeRh}_2\text{O}_5$                    | ICSD        | <i>Pnma</i>        | 4.16, 3.36, 3.57        |
| $\text{Ba}_2\text{CePtO}_6$                  | ICSD        | <i>Fm-3m</i>       | 3.66                    |
| $\text{Sr}_2\text{CeIrO}_6$                  | ICSD        | <i>P2_1/c</i>      | 4.63, 4.67, 4.66        |
| $\text{Ca}_2\text{CeO}_4$                    | Literature  | <i>Pbam</i>        | 4.41, 4.75              |
| $\text{CaCeO}_3$                             | OQMD        | <i>Pnma</i>        | 4.14, 4.35              |
| $\text{Sr}_2\text{CeSnO}_6$                  | OQMD        | <i>P2_1/c</i>      | 5.07, 4.92, 4.99        |
| $\text{Sr}_2\text{CeZrO}_6$                  | Literature  | <i>P2_1/c</i>      | 4.46, 4.44, 4.45        |
| $\text{SrCe}_{0.5}\text{Zr}_{0.5}\text{O}_3$ | Literature  | <i>Pnma</i>        | 4.63, 4.54, 4.55        |
| $\text{Sr}_2\text{CeHfO}_6$                  | Literature  | <i>P2_1/c</i>      | 4.56, 4.54, 4.55        |



# Publications/Presentations

## Publications (several in preparation)

- D. R. Barcellos, F. G. Coury, A. Emery, M. Sanders, J. Tong, A. McDaniel, C. Wolverton, M. Kaufman, and R. O'Hayre, *Inorg. Chem.* **58**, 7705 (2019)
- S S. Naghavi, J. He, and C. Wolverton, *CeTi<sub>2</sub>O<sub>6</sub>—A Promising Oxide for Solar Thermochemical Hydrogen Production*, *ACS Appl. Mater. Interfaces* (accepted)
- X. Qian, J. He, E. Mastronardo, B. Baldassarri, C. Wolverton, S.M. Haile, *Exceptional Stability and Favorable Redox Thermodynamics of Material for High-Capacity Solar Thermochemical Water Splitting*, Submitted, (2020).

## Invited Presentations (partial list)

- 2019 236th ECS Meeting
- 2019 American Chemical Society
- 2019 Materials Research Society
- 2019 Telluride Science Research Center Workshop
- 2018 TMS



# Proposed Future Work

- External validation of materials performance using DOE Nodes.
- Bulk measurements of generation 2 phase-change double perovskites.
- Establish thermodynamic properties of three 2<sup>nd</sup> generation systems.
- Thermochemical cycling measurements on the most promising materials.
- Refine computational approaches by feedback from experiments in Years 1 and 2 – extend to structure types beyond perovskite
- Focus computational work on promising phase-change compounds
- HydroGEN node collaborations on synthesis and characterization of additional computationally predicted compounds



# Project Summary

- Experimentally measured the enthalpy and entropy of predicted twelve perovskites and validated the high-throughput DFT calculation approach.
- Validated the high-throughput electrochemical impedance approach to extract redox thermodynamics by using gradient film.
- **High-Throughput Computational Survey of mixed perovskite phases resulted in prediction of compounds with promising thermodynamics**
- **Experimentally measured the thermodynamic properties of two predicted double perovskites and acquired high-capacity hydrogen productivity**